stellarator news

Published by Fusion Energy Division, Oak Ridge National Laboratory
Building 9201-2 P.O. Box 2009 Oak Ridge, TN 37831-8071, USA

Editor: James A. Rome Issue 64 July 1999
E-Mail: jar@ornl.gov Phone (423) 574-1306 Fax: (423) 576-3647
On the Web at *http://www.ornl.gov/fed/stelnews*

Long-pulse heating and plasma production by NBI in LHD

Negative-ion-based neutral beam injection (NBI) heating started in September 1998 in the Large Helical Device (LHD). In this first series of NBI heating experiments (the second experimental campaign in LHD), the achieved injection energy and power were 110 keV and 3.7 MW, respectively, using two injectors with a pulse duration of 0.6–2.0 s in core plasma experiments. Under these conditions, high stored energy (430 kJ), high plasma temperature (T_e = 2.3 keV), and long energy confinement time (0.26 s) were obtained.

Because the LHD coil system is made of superconducting magnets, in principle LHD has the ability to operate in steady state. Thus, long-pulse experiments aiming towards steady-state heating were performed with NBI in the second campaign. In most helical systems, neutral beams are usually injected into target plasmas produced with electron cyclotron heating (ECH) to provide additional heating. Unfortunately, because ECH utilizes a given EC resonance magnetic field, the magnetic field strength in experiments with ECH-produced plasmas is restricted to the resonant field. We achieved NBI-initiated plasma production for the first time in toroidal systems, thus eliminating this experimental constraint on the magnetic field strength.

We report the results of both long-pulse NBI plasma heating and plasma production. For both sets of experiments, the LHD magnetic field strength was 1.5 T and the major radius of magnetic axis was 3.75 m. The gas injected into the torus was helium.

Long-pulse NBI heating

One month after the start of injection, we achieved long-pulse plasma heating for 10 s with 80 keV and 1.1 MW of injected neutral beam using one co-injection beam line (BL2). The line-averaged electron density was gradually increased from 0.5 to 1.0×10^{19} m^{-3} and showed a rapid increase at around 8 s toward the pulse end. The stored

In this issue . . .

energy also increased towards the end of the pulse, corresponding to a confinement scaling with a positive density dependence. The central ion and electron temperatures were around 1.3 keV and decreased near the pulse end because of the density increase. At this time, the pulse duration was limited by beam blocking due to outgassing in the injection port, meaning the molybdenum protection plates in the injection port required more conditioning. At the end of the second campaign, by which time the injection port would have been conditioned, an NBI-heated plasma was sustained for 21 s in a quasi-steady state with a reduced injection energy and power of 0.6 MW at 66 keV, as shown in Fig. 1. The line-averaged electron density was almost constant in time at around 0.3×10^{19} m^{-3}, and the central ion temperature was also constant at around 1 keV. The radiation power was nearly stable, as were the impurity emission line intensities.

At higher densities, plasma oscillations were observed for 20 s, where the plasma density, the plasma temperature, and the impurity radiation all oscillate with a period of 1–3 s. During this 20-s period, observation of the plasma via a visible TV monitor with a tangential line of sight revealed alternate expansion and contraction, similar to "breathing." The shrinking and expanding correspond to decreases and increases in the electron temperature, respectively. Figure 2 shows the time evolution of various plasma parameters for the "breathing" relaxation oscillation plasma. During an increase in the line-averaged electron density, the density profile gradually becomes centrally peaked. However, the profile rapidly becomes flat or hollow during a decrease in density, similar to the density clamping phenomenon observed in short-pulse shots. The electron and ion temperatures start to increase a little before the density peak, and show a maximum a little before the density reaches its minimum. In a density

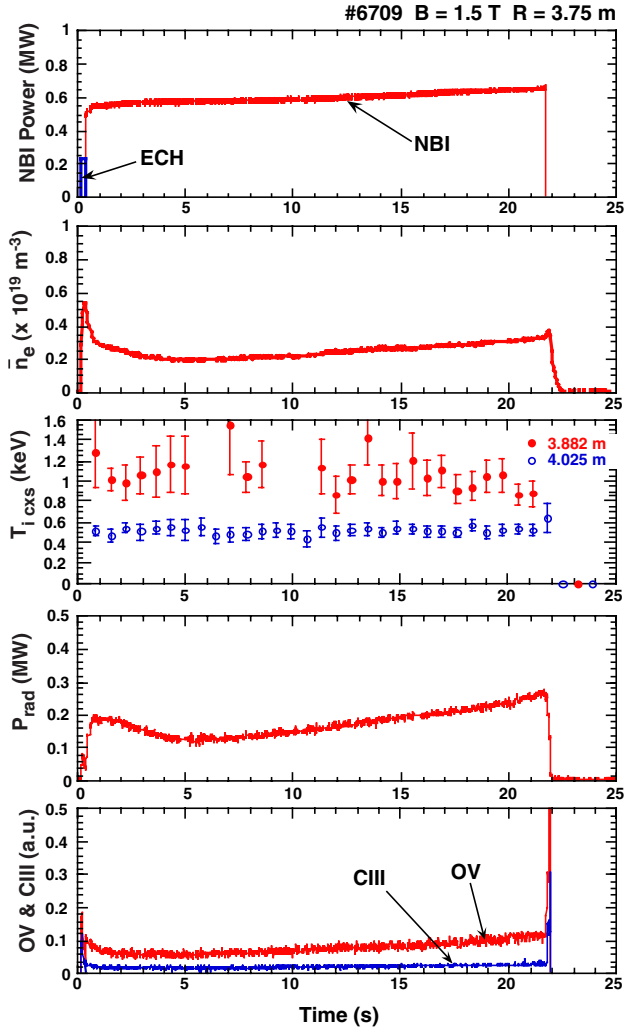

Fig. 1. Time evolution of various plasma parameters for the 66-keV, 0.6-MW, 21-s shot.

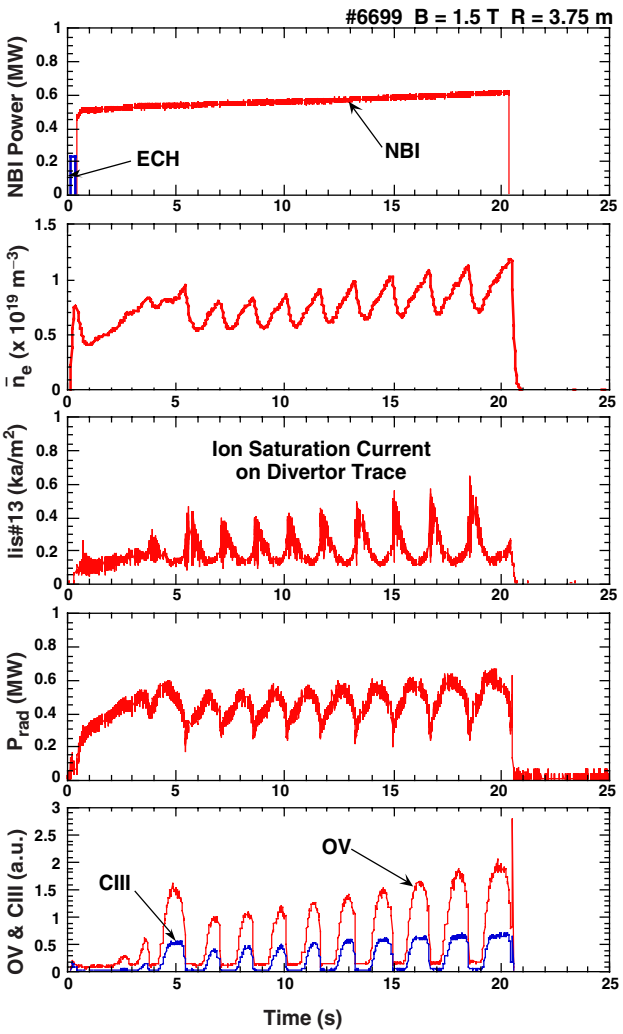

Fig. 2. Example of a relaxation oscillation plasma shot lasting for 20 s.

clamping (decreasing) phase, an increase in divertor flux is observed on electrostatic probes measured at a divertor trace. The impurity emission lines of O V and C III show larger intensities at a period of the density increase, i.e., the temperature decrease. The mechanism of this "breathing" phenomenon is under study.

Plasma production by NBI alone

Figure 3 shows an example of NBI plasma production. The beam energy was 97 keV. At a low background gas pressure of 10^{-3} Pa, the plasma is initiated and gradually built up to 10^{18} m^{-3} during several hundred milliseconds by NBI alone. Then, with a proper amount of gas puffing, high-stored-energy plasmas are obtained. The NBI-produced plasmas show the same characteristics as do those with ECH target plasmas. Part of the injected neutrals are ionized by collisions with the background gas, and the generated high-energy ions ionize the background neutrals. The high-energy ion density is determined by both the ionization cross section of the injected neutrals and the neutralization cross section of the high-energy ions due to collisions with the background gas. At higher injection energies (above 100 keV), the former cross section is much higher than the latter. Therefore, efficient NBI plasma production would require higher injection energy.

These results for long-pulse heating and plasma production show the unique characteristics of a helical system where the confinement magnetic surface is produced by external coils alone, independent of the plasma properties. Moreover, good confinement of high-energy ions ionizing the background gas is also indicated in the NBI plasma production experiment. In the third experimental campaign, starting in July, the injection energy will be raised to 150–160 keV by widening the beam acceleration gap length of negative ion sources. As a result, the injection power is expected to increase to 8 MW. Accordingly, 1-MW, 60-s NBI heating is projected.

Yasuhiko Takeiri for the LHD Team
National Institute for Fusion Science
Toki, Japan
E-mail: takeiri@LHD.nifs.ac.jp

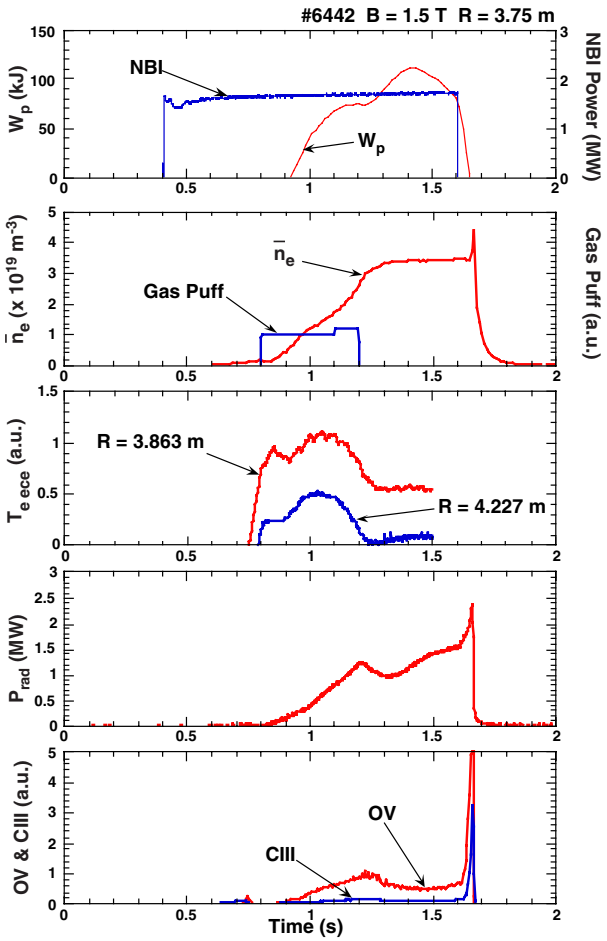

Fig. 3. Example of an NBI-produced plasma shot.

Physics optimization of a quasiomnigeneous stellarator*

Compact Stellarators with plasma aspect ratios $A_p = \langle R \rangle / \langle a \rangle = 2$–4 are of interest because they may combine the best features of tokamaks (moderate aspect ratio, good confinement and beta) and stellarators (disruption immunity, no current drive, low recirculating power in a reactor). Here $\langle R \rangle$ and $\langle a \rangle$ are the average major and minor radii of the plasma. The benefits of lower A_p are larger plasma size for a given cost for an experiment and lower cost for a given fusion power in a reactor.

Two complementary approaches are being studied for Compact Stellarators. Quasiaxisymmetric stellarators [1] have tokamak-like symmetry properties and bootstrap current comparable to that in a tokamak. The quasiomnigeneous (QO) stellarators [2] examined here use a spectrum of magnetic field spatial harmonics to minimize the deviation of bounce-averaged drift orbit (approximate second adiabatic invariant J^*) surfaces from magnetic surfaces (Fig. 1). The approximate alignment of drift surfaces with flux surfaces reduces energetic orbit losses and neoclassical transport. The low bootstrap current, typically ~1/10 that in a comparable tokamak, should lead to configurations that are relatively insensitive to beta and are robust against current-driven modes (external kinks), vertical instabilities, and disruptions.

Quasiomnigeneous stellarator optimization

QO stellarators have some general similarity to the drift-optimized Wendelstein 7-X (W7-X) "helias" configuration [3], but QO configurations have plasma aspect ratios smaller by a factor of 3–4, a significant bootstrap current, a larger helical component, and a smaller mirror-like variation of the magnetic field on a flux surface. Although the W7-X configuration has very attractive physics properties, it leads to a large ($\langle R \rangle = 22$ m) reactor. Compact QO configurations are of interest because they could lead to reactors with a volume-average beta $\langle \beta \rangle = 4$–5% and $\langle R \rangle \sim 9$ m, closer to the reverse-shear ARIES-RS tokamak reactor in the ratio of reactor mass to generated power.

The optimization criteria for QO configurations are their confinement properties, beta limits, and feasibility of the modular coil set. The goals are (1) energy confinement times $\tau_E > 2\tau_E^{ISS95}$, where τ_E^{ISS95} is the empirical stellarator confinement scaling [4]; (2) $\langle \beta \rangle \sim 4\%$ (for a reactor); and (3) modular coils with sufficient access for heating and diagnostics. Previously, the iterative optimization loop calculated the shape of the last closed flux surface (LCFS) that produces the desired physics properties using measures of trapped particle confinement (poloidal variation of B_{max}, B_{min}, J^*), beta limits (global magnetic well, Mercier stability), magnetic field ripple, outer surface curvature, and limits on the total current and rotational transform ι (= $1/q$) profiles. Figure 1 shows the type of improvement obtained as a result of the optimization procedure; the flux surfaces are concentric circles in this magnetic coordinate system. Similar improvements are obtained for passing particles, but the drift surfaces in the $v_\parallel/v$ range where orbits change from helically trapped to passing are not as well confined, and these determine the neoclassical transport.

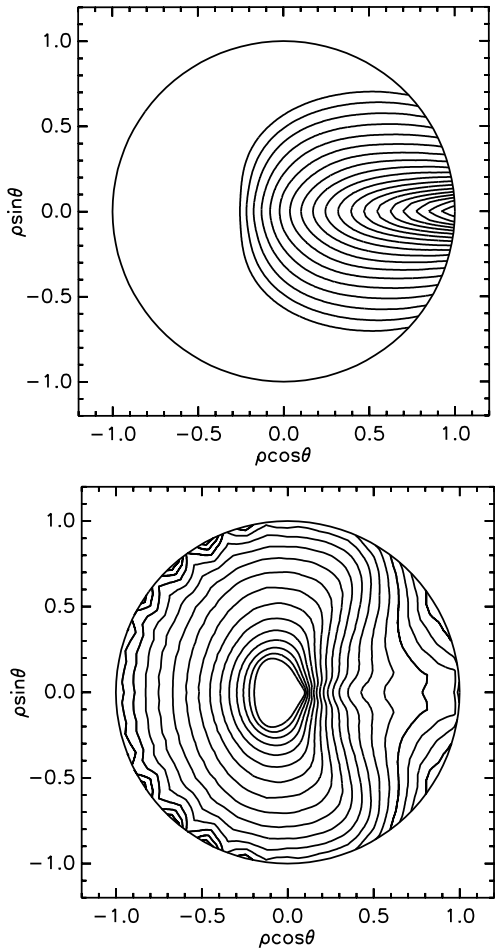

Fig. 1. J^* contours for helically trapped particles are open (top) before and closed (bottom) after optimization.

Different QO configurations are obtained depending on whether one is optimizing for (1) a reactor (where the critical issues are maximizing the space between the LCFS and the center of the coil winding surface, $\langle \beta \rangle$, and alpha particle confinement) or (2) a modest ($\langle R \rangle \sim 1$ m, $B \sim 1$ T, $P < 2$ MW) concept exploration experiment designed to test the physics of the approach (where confinement and configuration flexibility are more important issues). We have studied both optimizations, but here we are dealing primarily with the experimental optimization.

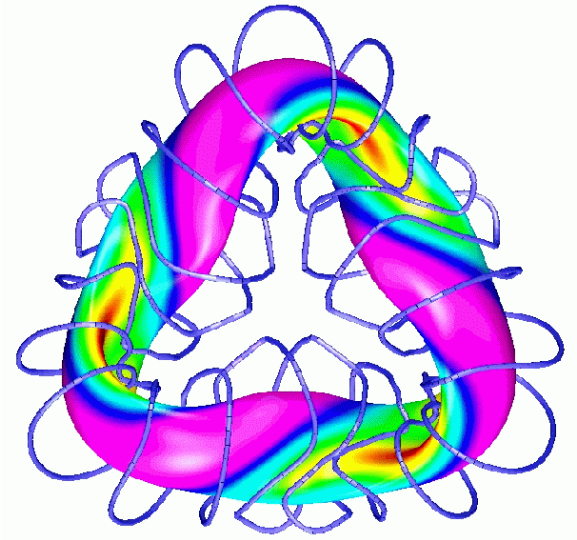

Fig. 2. LCFS and coils for an N_{fp} = 3 case.

QO-optimized configurations with toroidal field periods N_{fp} = 3 and 4 and A_p from 3 to 4.8 were examined. Figure 2 shows the LCFS for an N_{fp} = 3, A_p = 3.6 QO configuration optimized for an experiment and the modular coil set that creates it. Additional coils (not shown) are needed for configuration flexibility. The colors indicate contours of constant |*B*|. Figure 3 shows the spatial Fourier spectrum of |*B*| components for this configuration. The largest components are the helical, axisymmetric "1/*R*" term (a factor of 4 smaller than in an equivalent tokamak) and "bumpy" (mirror) terms. The spectrum of smaller compensating field terms is that needed to satisfy the physics constraints at lower aspect ratio. The on-axis field is normalized to 1 on this scale and the rotational transform varies from ι_0 = 0.55 on axis to ι_a = 0.64 at the plasma edge.

QO optimization reduces neoclassical transport because cross-field drifts scale with $\langle v_d \bullet \nabla\psi \rangle \propto \partial J^*/\partial\theta$, where v_d is the particle drift velocity, ψ is the flux, and θ is the

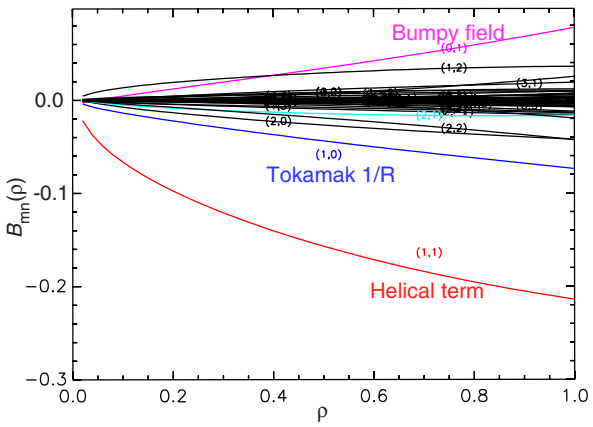

Fig. 3. Magnetic field structure for plasma in Fig. 2.

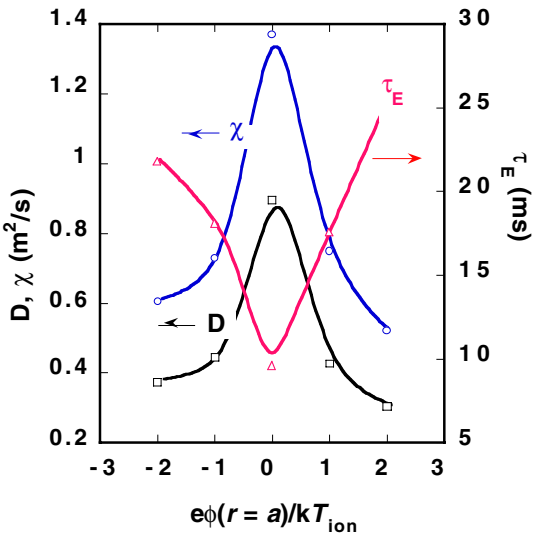

Fig. 4. Dependence of transport on the radial electric field.

poloidal angle. Figure 4 shows the result of a Monte Carlo calculation of the particle diffusivity D and heat diffusivity χ for an N_{fp} = 4, A_p = 4.2 QO configuration. It was obtained by following four groups of 2000 test particles with energies 0.5, 1, 2, and 3 keV in a background plasma with 1-keV temperature and 5×10^{19} m^{-3} density with different radial electric fields. The results were integrated over a Maxwellian distribution and the zero-dimensional (0-D) energy confinement time $\tau_E = \langle a \rangle^2/4\chi$, where χ was obtained from the energy moment in the integration. The values for D and χ decrease with decreasing density (and collisionality ν^*) and do not exhibit the $1/\nu*$ transport scaling normally associated with ripple-induced losses. For comparison, $2\tau_E^{ISS95}$ is 11.4 ms at P = 2 MW, about the same as the neoclassical value with no ambipolar electric field.

Energetic orbit confinement is important for heating schemes that rely on these particles in an experiment and for adequate alpha particle confinement in a reactor. The compatibility of QO configurations with ion cyclotron range of frequencies (ICRF) heating has been simulated in two ways. To simulate an experiment with energetic tail ICRF heating, 20-keV ions were launched at their turning points at the field resonance and followed collisionlessly. The loss rates were less than those for the CHS experiment in which ICRF heating was used successfully. Monte Carlo calculations have also started using a quasilinear ICRF diffusion operator to follow particles as they diffuse up in energy, allowing study of fundamental as well as minority tail ICRF heating. Following 500 3.5-MeV alpha particles for a reactor-scale version indicates an energy loss rate of ~20%, which is marginally acceptable for this application.

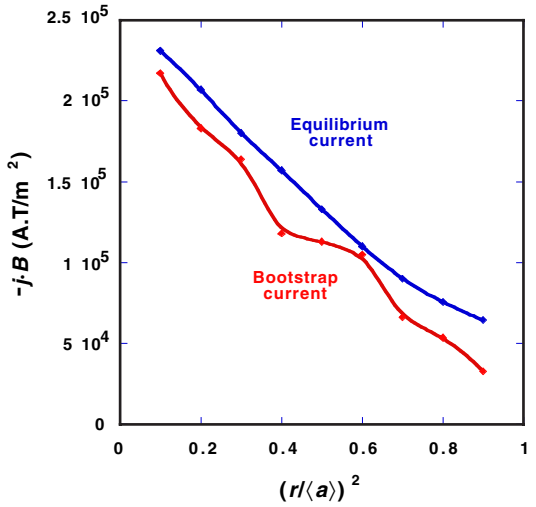

Fig. 5. QO bootstrap current profiles.

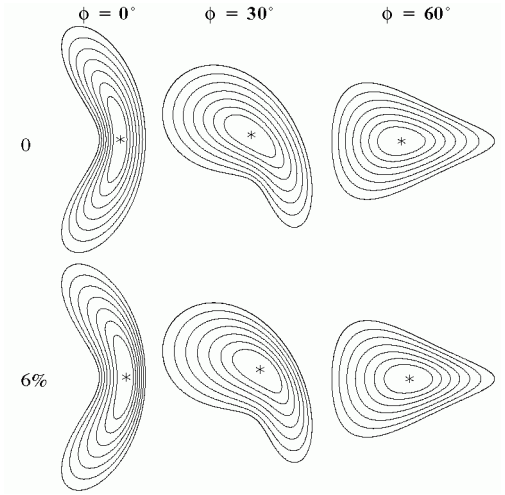

Fig. 6. Insensitivity of the plasma to increasing beta (0, 6%).

Optimization improvement

The development in the last year of much improved QO configurations with a stronger physics basis is due to incorporation of much faster (factor of ~10) calculations of both the self-consistent bootstrap current and the ballooning stability limit within the iterative optimization loop. The fast 3-D bootstrap code BOOTSJ has allowed determination of QO configurations with self-consistent bootstrap current. Figure 5 shows the radial variation of the bootstrap current from BOOTSJ and the VMEC [5] equilibrium solver that computes the magnetic field, metric elements, and other relevant surface quantities for a modified $N_{fp} = 3$, $A_p = 3.6$ QO configuration that is ballooning and Mercier stable at $\langle\beta\rangle = 2\%$. The bootstrap current is
−19 kA for the assumed density and temperature profiles. This is much smaller than the 380-kA plasma current in a tokamak with equivalent cross section and rotational transform. The current is not in the direction to stabilize neoclassical islands and tearing modes, but is thought to be sufficiently small to have little effect. Stability against external kinks or vertical instability is also expected for the same reason, but calculations are underway to check this.

QO configurations are relatively insensitive to changes in $\langle\beta\rangle$. Figure 6 shows the plasma cross sections at the beginning, one-quarter of the way and halfway through a field period for $\langle\beta\rangle = 0$ and 6%. There is little outward shift of the magnetic axis; the small bootstrap current produces only a small (~10%) change in $\iota(r)$.

Although the modest concept-exploration-level experiment discussed thus far would be power limited to $\langle\beta\rangle < 2\%$, higher values of beta ($\langle\beta\rangle > 4\%$) are needed for an attractive reactor. Ideal ballooning modes rather than kink modes set the critical $\langle\beta\rangle$ for QO stellarators because the bootstrap current is rather small, typically on the order of a few tens of kiloamperes. Ballooning instabilities are local modes that are driven unstable by the presence of pressure gradients in regions of bad local curvature. Their stabilization is difficult because their behavior is governed by local quantities such as the local shear or the local curvature. COBRA [6] has been developed to evaluate the ballooning growth rate on a prescribed set of flux surfaces and initial points for a given equilibrium. Integration of COBRA into the configuration optimization code has resulted in configurations with twice the value of $\langle\beta\rangle$ while preserving good transport properties. Figure 7 shows how the $N_{fp} = 3$, $A_p = 3.6$ QO configuration in Fig. 2 was modified to be stable at $\langle\beta\rangle = 3\%$. Figure 8 shows the modification of the original (unstable) configuration to the final (stable) configuration in the vertically elongated cross section. The rotational transform profile also changed at $\langle\beta\rangle = 3\%$ from nonmonotonic to monotonically increasing with radius. Small changes in the pressure profile used in Fig. 7 gave balloon-

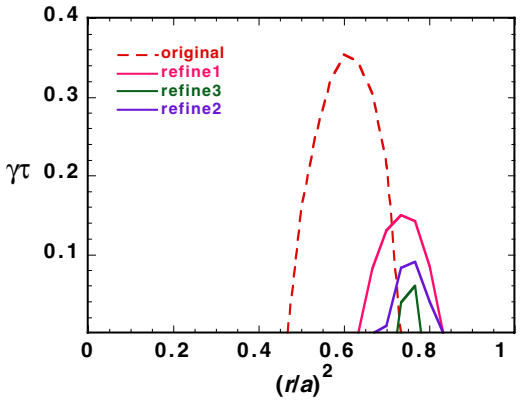

Fig. 7. Reduction of ballooning growth rate at $\langle\beta\rangle = 3\%$.

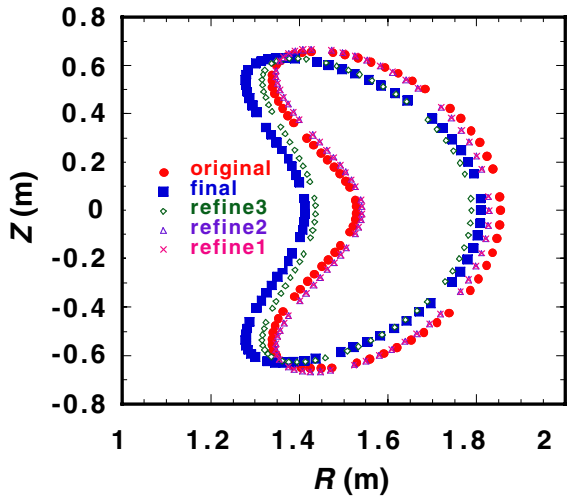

Fig. 8. LCFS changes corresponding to Fig. 7.

ing stability at $\langle\beta\rangle > 4\%$ for this final configuration. Newer configurations with higher rotational transform ($\iota_0 = 0.78$, $\iota_a = 0.91$) are also ballooning stable at $\langle\beta\rangle = 4\%$ with good confinement and small self-consistent bootstrap current. Earlier reactor-scale QO configurations had $\langle\beta\rangle$ up to ≈7%, good confinement, and a low bootstrap current contribution to ι, but the bootstrap current in those cases was not self-consistent with the MHD equilibrium.

Two improved measures of confinement are planned in the QO configuration optimization code. The approximate adiabatic invariant J^* (calculated by integrating $v_{||}$ along the toroidal angle in magnetic coordinates) will be replaced by the more accurate second adiabatic invariant J (calculated by integrating $v_{||}$ along the magnetic field) and extended to passing particles for a better calculation of orbit losses. A measure of local diffusive transport will be calculated in the optimization loop with the DKES (drift kinetic equation solver) code [7].

Nonplanar modular coils that accurately create the desired LCFS with adequate distances between the plasma and the coils, and between adjacent coils for heating and diagnostic access, were found (Fig. 2) by iteratively varying the parameters describing the coils until the desired match with the LCFS was obtained. The next step in improving the coil optimization code is to add constraints on the minimum bend radius and the distance between coils for finite cross-section coils. The distance between the LCFS and the center of the coil winding surface and the ratio of B_{max} on the coils to B_0 on axis will be optimized for studying the reactor extrapolation.

J. F. Lyon, S. P. Hirshman, D. A. Spong, R. Sanchez, L. A. Berry,
J. C. Whitson, D. B. Batchelor, J. Carlsson, B. E. Nelson
Oak Ridge National Laboratory, Oak Ridge TN 38731-8072 USA
E-mail: Lyonjf@fed.ornl.gov

References

[1] A. Reiman et al., IAEA-F1-CN-69/ICP/06, Proc. 17th IAEA Conf., Yokohama (1998).

[2] D. A. Spong et al., IAEA-F1-CN-69/ICP/07, Proc. 17th IAEA Conf., Yokohama (1998).

[3] J. Nührenberg and R. Zille, *Phys. Lett. A* **129**, 1139 (1988).

[4] U. Stroth et al., *Nucl. Fusion* **36**, 1063 (1996).

[5] S. P. Hirshman and J. C. Whitson, *Phys. Fluids* **26**, 3553 (1983).

[6] R. Sanchez et al., submitted to *J. Comput. Phys.* (1999).

[7] S. P. Hirshman and W. I. van Rij, *Phys. Fluids B* **1**, 563 (1989).

* Research supported by the U.S. Department of Energy under contract DE-AC05-96OR22464 with Lockheed Martin Energy Research Corp.

Initial experimental study of the "natural" helical divertor configuration in LHD

Edge plasma control using the divertor to improve the core plasma performance is one of the major experimental goals in LHD. Several divertor concepts, such as a local island divertor, are being discussed and will be prepared for application to LHD. In the first and second experimental phases (31 March – 31 May, 16 September – 31 December 1998), all experiments were performed under the open helical divertor (HD) configuration, which occurs naturally in a heliotron. An HD configuration can be characterized by its nonaxisymmetric structure and the existence of an ergodic region surrounding the core plasma [1]. In this study, plasma properties in the divertor and the ergodic regions, and their influences on the core plasma behavior, were investigated experimentally.

To measure the divertor plasma, a 21-channel Langmuir probe array was set on a carbon divertor plate located at the torus inboard side. At this location the magnetic surfaces are horizontally elongated, and we expect to detect two divertor channels as predicted by magnetic tracing calculations. The spatial resolution of the Langmuir probe array was designed to be 5 mm at its finest part to detect the narrow divertor channels. Profiles of ion saturation current, that is, particle flux (Γ_{div}), electron density ($n_{e,div}$), and temperature ($T_{e,div}$) were measured for various discharges using the single probe method. Electron temperature profiles in the ergodic region were obtained by a YAG Thomson scattering system. Electron density profiles were deduced from FIR interferometer measurement.

The temporal evolution of a typical hydrogen discharge with neutral beam injection (NBI) heating is shown in Fig. 1. NBI input power was 2.5 MW. In Fig. 1(a), strong density reduction is shown at t = 0.55 s in spite of continuous gas puffing. After the beginning of a rapid rise of the electron temperature in the ergodic region, the average density starts to decay. This density reduction was frequently observed in hydrogen discharges, and increasing the density by gas puffing was difficult. In helium discharges, this phenomenon was not strong. One possible cause of this density reduction is "screening" of fueling particles in this region. In LHD, the scale of the ergodic region is much larger than that of middle-sized devices, such as Heliotron-E and CHS. A calculation of magnetic field tracing shows that the width of this region is about 30 cm near the X-point and 4 cm even on the high-field side in the case of R_{ax} = 3.75 m. As shown in Fig. 1(c), $T_{e,edge}$ (at ρ = 1) is higher than 200 eV, and $n_{e,edge}$ obtained from FIR interferometer measurement is about half of the central density, that is, on the order of 10^{19} m^{-3}. Thus, fuel or

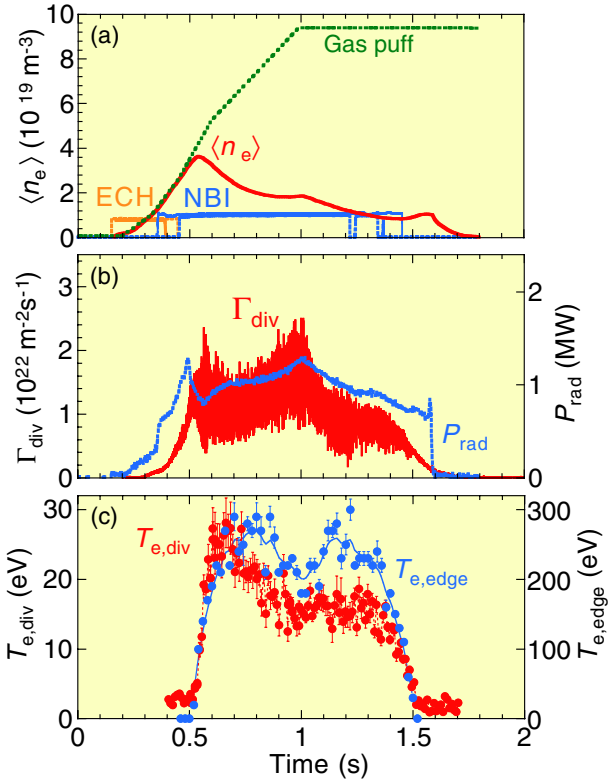

Fig. 1. Time evolution of a typical NBI-heated hydrogen discharge. P_{NBI} = 2.5 MW (port through), B_t = 1.5 T. (a) Line-average density and integrated fueling particle number. (b) Divertor particle flux and total radiation power. (c) Electron temperature in divertor and at the position of ρ = 1.

recycled particles can be ionized in this region, and they flow to the divertor along open field lines. In this phase, a particle source is found to exist in the ergodic region from the radial profile of the H_α intensity [2]. Due to this ion source in the ergodic region, Γ_{div} is increased even though the average density is reduced. In the case of relatively low electron temperature (< ~150 eV at ρ = 1), no density reduction was observed. Since atomic processes are considered to play an essential role for screening, density reduction appears to depend on the electron temperature in the ergodic region.

Figure 1(c) indicates that $T_{e,edge}$ is about 10 times higher than $T_{e,div}$. As mentioned, $n_{e,edge}$ is of the order of 10^{19} m^{-3}, and $n_{e,div}$ is typically below 1×10^{18}m^{-3}. These parameters indicate that plasma pressure is greatly reduced between the edge and the divertor through the ergodic region as observed in the case of a MARFE or detachment in tokamaks. We believe that tokamak cases and the LHD case differ because the region of pressure loss is localized in tokamaks, whereas it extends like a "mantle" in LHD. Momentum loss due to plasma-neutral interaction is strong in the ergodic region

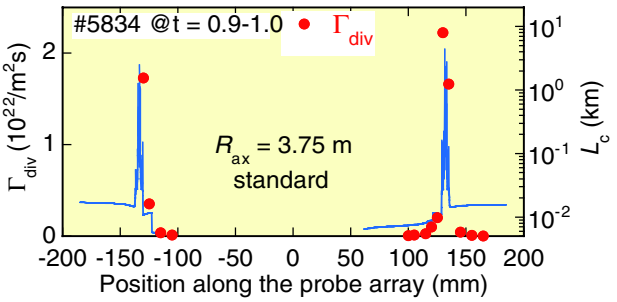

Fig. 2. Profiles along the Langmuir probe array of divertor particle flux and the connection length of magnetic field lines.

with its long open magnetic field lines (as discussed below), and this may cause this plasma pressure reduction.

Figure 2 shows profiles of Γ_{div} at t = 0.9–1.0 s in Fig. 1 and magnetic field connection length, L_c, obtained by calculation of magnetic field tracing along the Langmuir probe array. L_c at ±130 mm exceeds 1000 m, which is much longer than in large tokamaks. These long field lines run in the ergodic region surrounding the last closed flux surface (LCFS). Aside from these long field lines, L_c is shorter than a few tens of meters, and these lines run out of the edge surface layer [1].

Two peaks of Γ_{div} were observed at the positions of long magnetic field lines, which form divertor channels as expected. The extent of the Γ_{div} profile was found to be less sensitive to plasma parameters and strongly restricted by the magnetic field structure. These results seem to agree with calculations of magnetic field line tracing that included a random walk process [1]. The same results were obtained in discharges with a different magnetic axis.

Though the Langmuir probe array was set at only one location in the nonaxisymmetric structure of the HD, it is important to estimate the total particle and heat flux to the divertor. The divertor wet area, A_{div}, can be assumed to be 1.6 m^2 considering the total length of divertor trace on the divertor plate, ~160 m, and the width of the Γ_{div} profile, ~ 1 cm, obtained from the results of Langmuir probe array measurements. Uniformity of the divertor plasma is also assumed. The particle confinement time τ_p can be estimated as $\tau_p = \langle n_e \rangle V / S_{out}$, where V is the plasma volume (about 30 m^3 in LHD) and S_{out} is the outward flux from the core plasma. The latter can be considered to be equal to ($\Gamma_{div} A_{div}$). In Fig. 1(a), the average density is 3.6 × 10^{19} m^{-3} at t = 0.55 s, and S_{out} = ($\Gamma_{div} A_{div}$) = (1.6–2) × 10^{22} s^{-1}. Thus τ_p is calculated to be 54–67 ms, and it is less than τ_E [3]. The existence of a particle source in the ergodic region might influence this result.

The divertor heat flux, Q_{div} (W/m^2), is estimated using the measured Γ_{div} and $T_{e,div}$ as $Q_{div} = \gamma (\Gamma_{div} T_{e,div})$, where γ is the heat transmission factor in the electrostatic sheath formed in front of the probe array and is assumed to be 7 ($T_{e,div} = T_{i,div}$ is assumed). Q_{div} is estimated to be (0.2–0.28) MW/m^2 at t = 0.55 s in Fig. 1. The total power flux to divertor region may be estimated as ($Q_{div} S_{div}$), which yields 540 kW, and the total radiation power is 800 kW at t = 0.55 s. The sum of these is about half of the deposition energy. One cause of this difference between input and loss power is considered to the assumptions mentioned above, and atomic processes also seem to play an important role.

In HD configuration experiments, understanding the plasma behavior and atomic processes in the ergodic region are considered to be essential to understanding the core plasma properties. In the next experimental term (16 July – 16 December 1999), a reciprocating Langmuir probe system and lithium beam probe system will be used to obtain detailed measurements of plasma parameters in the ergodic region. Six Langmuir probe arrays have been installed in typical divertor plate positions to clarify the 3-D structure of divertor traces in the HD configuration.

S. Masuzaki for LHD experimental groups
National Institute for Fusion Science
Oroshi 322-6, Toki 509-5292, Japan
Phone: +81-572-58-2145
Fax: +81-572-58-2618
E-mail: masuzaki@LHD.nifs.ac.jp

References

[1] N. Ohyabu et al., *Nucl. Fusion* **34**, 384 (1994).

[2] S. Morita et al., Proc. 26th EPS Conference., Maastricht (1999).

[3] O. Motojima et al., *Phys. Plasmas*, **6**, 1843 (1999).

Experimental plan for the third LHD campaign

The schedule of the third experimental campaign of LHD is shown in Fig. 1. For this campaign, experiments will be conducted at a magnetic field of >2.5 T with gradually increasing heating power, aiming at producing plasmas with a higher temperature and higher density than ever. The total ECH power, injected through three ports, is planned to be 1 MW using six gyrotrons, since two transmission lines are installed in each port. The neutral beam injection (NBI) energy will be increased to 180 keV, and the injection power raised to several megawatts. For the ICRF heating experiments, a folded waveguide antenna, installed after the second experimental campaign for ion Bernstein wave heating, allows plasma production to be done independently of the magnetic field. The expected loading power is 0.5 MW for 1 s, which will be increased to 1 MW for 10 s. ICRF heating experiments with a power of 0.35 MW for 0.2 s also started in the second campaign, using one pair of fast wave antennas for electron/ion heating. The loading power expected for these fast wave antennas in the third experimental campaign is 1 MW for 10 s. The excitation test to the rated field of 3 T is planned after the third experimental campaign.

The vacuum test of the cryostat began on 17 May 1999. The cryostat, which has a volume of 580 m^3 and an extended surface of about 70,000 m^2, was evacuated within a day, and the pressure reached about 0.03 Pa, low enough for the cooldown of LHD. No leak was found in the cryostat in the range of 10^{-8} Pa m^3/s. The vacuum test of the plasma vacuum vessel began on May 31, and several small leaks were found during the helium leak test. These were plugged, and no leak remains in the plasma vacuum vessel in the range of 10^{-9} Pa m^3/s. The pressure in the plasma vacuum vessel reached 9×10^{-7} Pa in the middle of June.

We started the main compressors on June 2 and continued the purifying of the cryogenic system until June 9 to remove impurities in the helium gas (e.g., oxygen, nitrogen, and water). The cooldown of LHD started on June 10. At first the superconducting coils, supporting structures, and 80 K shield were cooled by helium gas, the temperature of which was controlled by mixing cold and warm gases in order to keep the temperature differences in the coils and the supporting structures to less than 50 K. This temperature distribution determines the cooling rate. Below 85 K, seven turboexpanders were put into operation. The helical coils, poloidal coils, and superconducting bus lines are expected to go superconducting at the beginning of July. The third experimental campaign will start after two days of coil current excitation tests to produce fields of up to 2.5 T.

O. Motojima
Director, Department of Large Helical Device Project
National Institute for Fusion Science
322-6 Oroshi-cho, Toki 509-5292, Japan
E-mail: motojima@LHD.nifs.ac.jp

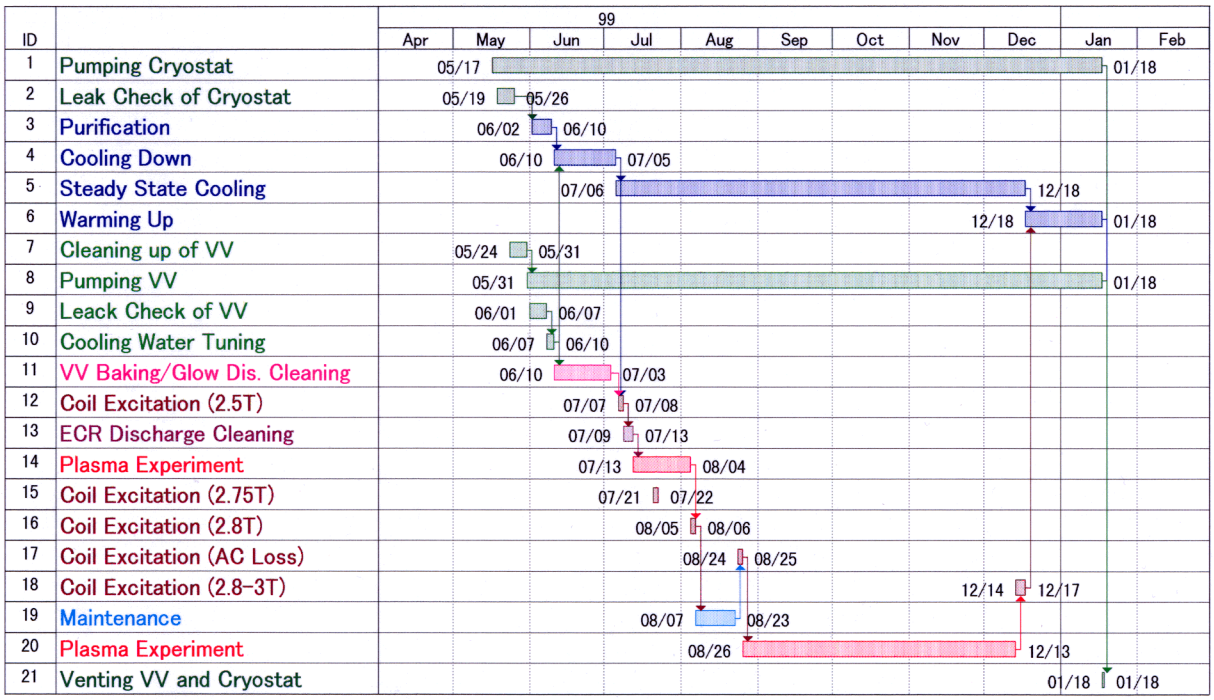

Fig. 1. Schedule for third experimental campaign in LHD.

10th International Toki Conference on Plasma Physics and Controlled Nuclear Fusion (ITC-10)

"Physics and Technology for Steady State Plasmas"

Organized by National Institute for Fusion Science, January 18–21, 2000
Ceratopia Toki Conference Hall, Toki City, Japan

The International Toki Conference on Plasma Physics and Controlled Nuclear Fusion (ITC) was initiated in 1989 when the National Institute for Fusion Science (NIFS) was established. Since then, the ITC has been held annually at Toki City. Each year's conference has focused on a current fusion/plasma topic of the year. "Physics and Technology for Steady-State Plasmas" has been chosen as the main topic of this year's ITC.

During the two decades since the 1970s, great progress has been achieved in nuclear fusion research. High-temperature (10 keV) plasmas have been realized, demonstrating a reactor-relevant plasma core. However, these high temperatures can be sustained for only a few seconds at present, which is still far from the requirements of a reactor. Since the achievement of 10 keV, it has been recognized that the long-pulse, steady-state maintenance of this plasma is one of the next major milestones.

Now research activities are being accelerated toward the goal of long-pulse operations with the start of experiments in the superconducting helical device, LHD. This conference is planned at this opportunity, in order to stimulate research activities in this direction and to get a clearer view of the issues related to this problem.

It is important to take another look at ongoing studies that are focussed on long-pulse, high-power operation along with studies directly addressing steady-state operations. We welcome contributions from many scientists and engineers working in the various fields of fusion research.

Conference Topics

- Ongoing studies and near-term plans for steady-state operation in fusion experimental devices
- Heating systems for long-pulse, steady-state operation
- Fueling, exhaust, particle balance and control
- Heat removal and high-heat-flux components
- Edge plasma and divertor physics in tokamaks and helical devices
- Plasma-facing materials and plasma-surface interactions (erosion/redeposition, hydrogen recycling, impurity generation, etc.)
- Equilibrium control in full steady-state operation
- Control of profiles such as density, pressure, $\mathbf{E} \times \mathbf{B}$ shear, current, etc.
- Physics issues favorable to long-pulse operations from theoretical viewpoints
- Diagnostics, data acquisition and control systems
- Magnets, facilities, and other technologies
- Reactor concepts and design studies

Date and place

The Conference will be held 18–21 January 2000, at the Ceratopia Hall in Toki City, which is located near Nagoya. The registration desk will open on 17 January.

Additional Information

More detailed information can be found at the conference Web site (http://www.nifs.ac.jp/~itc10/).

The IAEA Technical Committee Meeting on Steady State Operation of Magnetic Fusion Devices is to be held at Kyushu University in October 1999. We make an effort to share topics between the two conferences. We expect that the Toki Conference will shift its focus slightly towards alternative concepts.

Conference Secretary

Nobuaki Noda
National Institute for Fusion Science
Toki City 509-5292, Japan
Telephone: +81-572-58-2152
Fax: +81-572-58-2618
E-mail: ITC10@nifs.ac.jp
URL: http://www.nifs.ac.jp/~itc10/

12th International Stellarator Workshop

September 27–October 1, 1999

The International Stellarator Workshop is held every two years to focus on new results and ongoing activities in theory and experimental research in helical systems. With a number of new operating devices and worldwide interest in stellarator configurations for plasma containment, this should prove to be an exciting Workshop.

Topics

- Transport and confinement improvement
- MHD equilibrium and stability
- Plasma edge and turbulence
- Particle and power handling
- Divertors and impurity control/transport
- Plasma heating
- Diagnostics
- Configuration optimization
- New devices
- Reactor studies

Date and Place

The Workshop will be held 27 September–1 October 1999, at the Monona Terrace Convention Center in Madison, Wisconsin. Monona Terrace is a newly constructed structure designed by Frank Lloyd Wright and first proposed in 1938. The Center brings to life one of Wright's final creative visions in a spectacular lakeside setting. For information on Madison, tour the Web site:
http://www.visitmadison.com

Language

The working language for the Workshop is English.

Registration

If you plan to submit a paper or attend the Workshop, please fill out and return the registration form on the Web page by 26 August (fax or mail). Please note that to encourage advance registration for planning purposes, there is a substantial discount on the fees for registration by this date. Web-based registration is available for those wishing to pay by credit card or purchase order. The address is:
http://hsxa.ece.wisc.edu/Stell_Workshop

Additional conference information will be posted to the site as it becomes available. Registration fees include banquet, book of abstracts, proceedings on CD-ROM, and conference materials.

Deadlines and Contacts

Receipt of one-page abstracts - - - - - - - - 30 July 1999
Lodging Reservations - - - - - - - - - - 26 August,1999
Advance (discounted) registration - - - - 26 August 1999
Receipt of final papers - - - - - - - - 27 September 1999

Workshop Web site:
http://hsxa.ece.wisc.edu/Stell_Workshop
Program:
J. F. Lyon (lyonjf@fed.ornl.gov)
Local arrangements:
D. T. Anderson (dtanders@facstaff.wisc.edu)

U.S.-Japan Workshop on Stellarator/Helical System Concept Improvement

A U.S.-Japan Workshop on Stellarator/Helical System Concept Improvement will be held at Oak Ridge National Laboratory on 23 and 24 September, the Thursday and Friday before the International Stellarator Workshop in Madison. The focus of this smaller workshop (the third in a series) with researchers from Japan, the United States, and Europe will be new stellarator configurations and the physics behind them. Contact Jim Lyon for details and arrangements.

J. F. Lyon
Fusion Energy Division, MS 8072, Building 9201-2
Oak Ridge National Laboratory
P.O. Box 2009
Oak Ridge, TN 37831-8072, USA
Fax: +1-423-574-1191
Telephone: +1-423-574-1179
E-mail: lyonjf@fed.ornl.gov